PS C54

Characterisation of outward currents in muscle fibres from *Fasciola hepatica*

D. Kumar*, I. Fairweather†, C. White‡ and J.G. McGeown‡

‡*Smooth Muscle Research Group and* †*Parasite Proteomics and Therapeutics Research Group, Queen's University, Belfast BT9 7BL, UK and* **Division of Pharmacology and Toxicology, Indian Veterinary Research Institute, Izatnagar 243 122, Uttar Pradesh, India*

The liver fluke, *Fasciola hepatica*, relies on highly co-ordinated motor activity to enter and remain within the bile ducts of its host. Understanding the control of this mechanical activity may suggest new therapeutic strategies with which to combat these and similar parasites. Since mechanical activity in many muscle types is triggered by excitation of the cell membrane, we set out to characterise some of the relevant ionic currents.

Rats infected with *F. hepatica* were humanely killed and flukes were extracted from the biliary tree. Cells were isolated from the ventral suckers using successive incubations at 37 °C in Ca^{2+}-free Hedon-Fleig solution containing dithiothreitol (5 mM) and bovine serum albumin (0.1 %) to which papain (2 mg ml^{-1}) was added during the first incubation and trypsin (2 mg ml^{-1}) during the second. Muscle fibres were then released by gentle trituration in enzyme-free solution and superfused with Ca^{2+}-containing modified Hedon-Fleig solution at room temperature. They were voltage clamped using the perforated patch technique with amphotericin B (200 μg ml^{-1}) dissolved in K^+ (133 mM) pipette solution. The statistical significance of differences in summarised data (means ± S.E.M.) was assessed using Student's paired *t* test.

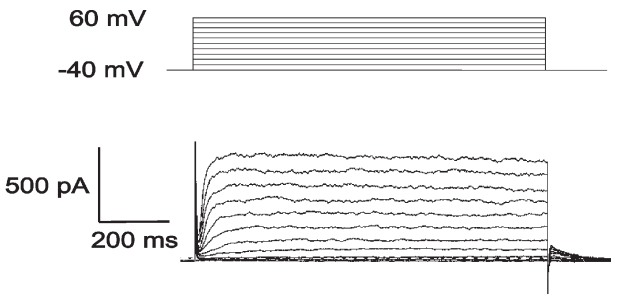

Figure 1. Outward currents recorded from a muscle fibre of the ventral sucker of *F. hepatica* (lower panel). Depolarisations were incremented in 10 mV steps from –40 mV to +60 mV (upper panel).

Depolarisation from a holding potential of −40 mV activated outward currents (Fig. 1). The kinetics of activation were voltage dependent, with the time required for the current to reach 80 % of its peak value falling from 57 ± 11 ms at 0 mV to 16 ± 2 ms at +60 mV ($P < 0.005$, $n = 7$). Tail currents recorded on repolarisation to different potentials after a 200 ms activation step to +60 mV reversed direction at −69 ± 3 mV under control conditions ($E_K = -89$ mV). This reversal potential shifted to −23 ± 1 mV when E_K was raised to −37 mV ($P < 0.00005$, $n = 6$). The deactivation kinetics of these tail currents were also strongly voltage dependent, the time required for 80 % decay falling from 123 ± 9 ms at −20 mV to 6 ± 1 ms at −110 mV ($P < 0.0001$, $n = 6$). The peak outward current was reduced by 77 ± 6 % in the presence of tetrapentylammonium chloride (1 mM; $P < 0.0005$, $n = 5$) and by 59 ± 4 % in the presence of nimodipine (30 μM; $P < 0.005$, $n = 7$).

These results suggest that voltage- and Ca^{2+}-sensitive K^+ currents are likely to play a role in shaping membrane potential changes in these cells.

D.K. was supported by an International Research Fellowship from the Wellcome Trust.

All procedures accord with current UK legislation

PS C55

Roles of molecular regions in determining activation kinetics of heag potassium channels

M. Ju and D. Wray

School of Biomedical Sciences, University of Leeds, Leeds LS2 9JT, UK

We have recently cloned the eighth member of the *ether-à-go-go* potassium channel family in human, heag2 (Ju & Wray, 2002). The activation kinetics of this channel are different from the closely related, homologous heag1 channel, which shows 73 % identity at the amino acid level. In this study, we have investigated the molecular regions that are involved in determining the differences in activation kinetics between heag1 and heag2 channels.

For this, chimaeras between heag1 and heag2 were constructed by restriction digest and subsequent ligation. Chimaeras were made by swapping amino acids 1–137 in the intracellular N terminal region, which includes the PAS domain, or by swapping amino acids 138–549, which includes the central transmembrane regions S1–S6. Constructs were expressed in *Xenopus* oocytes, and two-electrode voltage-clamp recordings were made 2 days later at room temperature. Test potentials were then applied to 0 mV (500 ms duration) from a holding potential of −80 mV, and activation times were measured as the time from 20 % to 80 % of maximal current. For each chimaera, wild-type recordings were carried out in the same batch to allow for variations between batches of oocytes.

Chimaera I with amino acids 1–137 of heag2 replaced by those of heag1 showed an activation time (19.0 ± 2.1 ms, $n = 10$, mean ± S.E.M.) that was not significantly different from that for heag1 wild-type (20.1 ± 6.0 ms, $n = 5$) but significantly faster than for heag2 wild-type (59.7 ± 12.7 ms, $n = 6$, $P < 0.05$, Student's unpaired *t* test). This indicates that amino acids contained within the region 1–137 are involved in determining differences in activation times between the two channels.

Chimaera II with amino acids 138–549 of heag2 replaced by those of heag1 displayed an activation time (21.1 ± 2.7 ms, $n = 8$) that was also not significantly different from that for heag1 wild-type (14.0 ± 3.1 ms, $n = 7$) but significantly faster than for heag2 wild-type (86.2 ± 9.5 ms, $n = 4$, $P < 0.05$). This suggests that amino acids within the region 138–549 are also involved in determining differences in activation times between heag1 and heag2.

Taken together, these results suggest that some amino acids within the intracellular N-terminal region (which includes the PAS domain), as well as some residues within the central region (which includes the membrane-spanning domains S1–S6), are involved in determining differences in activation kinetics between heag1 and heag2 channels. It seems likely that these effects on channel activation in heag occur because of an interaction between the N-terminal region with the membrane-spanning region.

Ju M & Wray D (2002). *FEBS Lett* **524**, 204–210.

All procedures accord with current UK legislation

PS C56

Inter- and intra-subunit interactions between the voltage-sensing S4 segment and the pore domain in the Shaker K^+ channel

D.J.S. Elliott, E.J. Neale, J. Dunham, M. Hunter and A. Sivaprasadarao

School of Biomedical Sciences, University of Leeds, Leeds LS2 9JT, UK

The Shaker K^+ channel is a member of the Kv channel family, made up of four subunits each comprising six membrane embedded segments (S1–S6): S1–S4 form the voltage-sensing domain and S5–P–S6 the pore domain. During depolarisation S4, the principal component of the sensor, moves out of the membrane bilayer, which leads to opening of gates situated in the pore domain. Using the engineered metal and disulphide bridge approaches, we have shown that residue S357 in the S3–S4 linker (3 residues from S4) lies close to residue E418 at the top of S5 of an adjacent subunit in the closed state of the channel (Neale *et al.* 2003). Here we have investigated the interactions of residues downstream of S357, with E418.

Cysteine mutations were introduced at positions 358–362 in Shaker-IR. A second cysteine was introduced at 418. Single and double cysteine mutant channels were expressed in *Xenopus* oocytes and currents measured by two-electrode voltage clamp. The effects of 100 μM Cd^{2+} on the properties of these channels were examined. Effects on the double mutant channels that were significantly different from those on the single mutant channels were interpreted as Cd^{2+} binding between the engineered cysteines, reflecting their close proximity.

Cd^{2+} caused significant conductance loss (35–80 %; $P < 0.05$, Student's unpaired t test) in 358C–418C, 360C–418C and 361C–418C double mutant channels, but not in the corresponding single mutant channels. These effects were seen only at depolarised potentials, indicating that depolarisation-induced conformational changes bring the engineered cysteines into close proximity. To investigate if Cd^{2+} forms a bridge between cysteines within the same subunit or from neighbouring subunits, we have made tandem dimer constructs, in which one cysteine was present in S4 of one protomer, and the second cysteine at 418 of the second protomer. The resulting constructs when expressed should form tetramers with the S4 and pore cysteines in diagonally located subunits. No effect of Cd^{2+} was seen on 360C–418C and 361C–418C tandem dimers, suggesting that the interactions require cysteines to be present in the same subunit. This is in contrast to the 357C–418C double mutant channel, where interactions between 357C and 418C, were found to be between the adjacent subunits.

Based on these data, we propose that the top of S4 moves from the top of S5 of a neighbouring subunit to its own subunit during gating, in a motion that involves a combination of vertical and horizontal translation. Such motions can be explained in terms of the recently solved structure of the archaebacterial Kv channel, KvAP (Jiang *et al.* 2003).

Jiang Y *et al.* (2003). *Nature* **423**, 33–41.

Neale EJ *et al.* (2003). *J Biol Chem* (in press).

This work was funded by the Wellcome Trust.

All procedures accord with current UK legislation

PS C57

Glucose-induced oscillations in cytosolic calcium in human embryonic stem cells

R.M. Shepherd*, K.E. Cosgrove*, L. Ruban†, A. Natarajan*, A.-M. Gonzalez*, H.D. Moore†, P.W. Andrew‡ and M.J. Dunne*

** School of Biological Science, Division of Physiology and Pharmacology, University of Manchester, Oxford Road, Manchester M13 9PT, † Department of Biomedical Science, University of Sheffield, Western Bank, Sheffield S10 2TN and ‡ Section of Reproductive and Developmental Medicine, University of Sheffield, Jessop Wing, Sheffield S10 2TN, UK*

Differentiated human embryonic stem cells potentially represent a limitless source of insulin-secreting cells for transplantation-based therapy for diabetes mellitus. We used embryoid bodies (EBs) derived from the pluripotent human embryonic stem cell line H7 (hES-H7), in order to examine mRNA expression profiles and to document cytosolic calcium ion signalling events relevant to those processes that are normally present in human pancreatic β-cells.

hES-H7 cell-derived EBs, maintained in suspension culture for 1–3 weeks, were used throughout these experiments. Comparative studies with human β-cells were made from adult, neonatal and fetal tissues obtained with informed consent and local ethical committee approval. Measurements of cytosolic Ca^{2+} signalling ($[Ca^{2+}]_c$) were performed with fura-2 imaging techniques. Total RNA was extracted from the EBs and primary tissue, and RT-PCR used to study the expression of mRNAs for ion channels, receptors and glucose transporters using specific oligonucleotide primers.

In hES-H7 EBs the resting $[Ca^{2+}]_c$ was $\sim 48 \pm 6$ nM ($n = 6$) compared to $\sim 62 \pm 3$ nM ($n = 102$) in small cell aggregates and isolated cells. This is lower than resting $[Ca^{2+}]_c$ measured in adult and neonatal human islets: 80 ± 5 nM ($n = 733$). In HES-H7 EBs, glucose induced the development of oscillatory responses in $[Ca^{2+}]_c$-raising the ambient $[Ca^{2+}]_c$ by ~ 25 nM ($n = 4$). In addition, KCl (40 mM, $n = 10$, $\Delta[Ca^{2+}]_c \approx 20$ nM), ATP (0.1 mM, $n = 9$, $\Delta[Ca^{2+}]_c \approx 50$ nM) and acetylcholine (0.1 mM, $n = 6$, $\Delta[Ca^{2+}]_c \approx 20$ nM) were each found to elevate $[Ca^{2+}]_c$. We also found that adult and neonatal human islets responded in similar ways to each of these agonists.

RT-PCR using the hES-H7 EBs revealed the expression of mRNAs encoding the GLUT-1 and GLUT-2 glucose transporters, the subunits of β-cell K-ATP channels, Kir6.2, SUR1, and the voltage-gated Ca^{2+} channel α-subunits CACNA1A, -B and -C, but not CACNA1D, all of which were detected in human adult and fetal islets at 13 weeks gestation. Additionally EBs were shown to express mRNAs for purinergic ($P2X_4$) and muscarinic (P2Y1, P2Y2, P2Y4 and P2Y6) receptor subtypes, unlike adult islets which expressed $P2X_4$ and P2Y1 only. ES-derived embryoid bodies represent a developmental progression towards production of mature cell types.

These studies have shown that hES-H7-derived EBs have the potential to respond to glucose due to expression of key stimulus–secretion coupling pathway proteins which are also found in adult human β-cells.

All procedures accord with current local guidelines and the Declaration of Helsinki

PS P134

Stimulus–secretion coupling mechanisms in human insulinoma β-cells

K.E. Cosgrove, A. Natarajan, R.M. Shepherd, E.M. Fernandez, A.T. Lee, A.-M. Gonzalez and M.J. Dunne

University of Manchester, School of Biological Sciences, Division of Physiology and Pharmacology, G38 Stopford Building, Oxford Road, Manchester M13 9PT, UK

Recent advances have revealed that hyperinsulinism in infancy is a disorder caused by loss of function of K-ATP channels (OMIM 600937, 600509). By contrast, little is known about the pathophysiology of human insulinomas, which are the most common cause of hypoglycaemia in adulthood.

Insulinomas were surgically removed from the pancreata of five patients and a controlled collagenase digestion procedure used to liberate single β-cells. Cells were maintained under standard tissue culture conditions in supplemented RPMI 1640 medium at 37 °C. Control human β-cells and islets were obtained from 56 cadaver organ donors. The function of K-ATP channels, voltage-gated Ca^{2+} channels (VGCC), and voltage-gated K^+ channels (VGKC) was assessed using patch clamp electrophysiology. Intracellular Ca^{2+} levels $[Ca^{2+}]_i$ were estimated using fura-2-loaded cells or islets with microfluorimetry or digital imaging techniques. Results are expressed as means ± S.E.M. and Mann-Whitney rank sum tests were used to test for statistically significant differences.

Total RNA was extracted from cells or islets and used for RT-PCR to determine expression of glucose transporter and ion channel subunit genes using specific oligonucleotide primers. Unlike control islets, insulinoma β-cells were found to exclusively express the GLUT1 facilitated glucose transporter and not a combination of both GLUT-1 and -2 mRNAs. SUR1 and Kir6.2 mRNAs were expressed in insulinoma β-cells, and K-ATP channel currents were consistently recorded from all five patient tissues ($n = 4$–46). Although peak currents following patch excision were reduced by ~50% ($P < 0.001$) when compared with control β-cells (11.6 ± 1.0 pA ($n = 106$, 5 patients) *vs.* 25.5 ± 1.5 pA ($n = 269$, 56 donors)), K-ATP channels responded normally to internally applied nucleotides (ATP 10 μM to 5 mM, ADP 500 μM, GDP 500 μM) and the K-ATP channel agonists diazoxide (10 μM to 500 μM), BPDZ 154 (10 μM) and NNC55-0118 (10 nM to 200 μM). Control human islets and insulinoma β-cells expressed VGCC subunit mRNAs for Cav1.2, 1.3, 2.1, 2.2, β2 and β3. Functional studies revealed that whilst there were no major differences in the magnitude of VGCCs (-11.8 ± 3.3 pA pF^{-1} ($n = 7$) *vs.* -9.2 ± 0.7 pA pF^{-1} ($n = 56$ from 10 donors, n.s.) at −10 mV from a holding potential of −80 mV), in one out of three patients there were marked increases in the basal cytosolic Ca^{2+} concentrations: 154 ± 12 nM ($n = 74$) *vs.* 80 ± 9 nM ($n = 677$ from 53 control donors, $P < 0.001$). We found no differences in the mRNA expression profiles of Kv α- and β-subunits, although VGKC currents were markedly increased in magnitude when compared to controls: 392 ± 50 pA pF^{-1} ($n = 6$, 1 patient) *vs.* 132 ± 9 pA pF^{-1} ($n = 40$ from 6 donors) at +80 mV from a holding potential of −70 mV ($P < 0.001$).

In summary, insulinoma β-cells selectively expressed the GLUT-1 glucose transporter, but there were no major alterations in the expression profiles or functions of K-ATP channels, VGKC or VGCC. Collectively, these data reveal that defects in glucose-regulated ion channels are unlikely to explain the general pathophysiology of inappropriate insulin release in human insulinomas.

All procedures accord with current local guidelines and the Declaration of Helsinki

PS P135

Expression of delayed rectifier potassium channel mRNAs and their function in human insulin-secreting cells

Eva M. Fernandez*, Karen E. Cosgrove*, Keith J. Lindley†, Mark J. Dunne*

** School of Biological Sciences, University of Manchester, Manchester and †Institute of Child Health, London, UK*

Pancreatic β-cells are electrically active cells and release insulin in response to glucose through marked changes in the cell membrane potential. The resting membrane potential is determined by the Na^+,K^+-ATPase pump and K_{ATP} channels. Following glucose metabolism, K_{ATP} channel closure facilitates a depolarisation of the membrane, leading to the opening of voltage-gated calcium channels, and insulin is released as a consequence of Ca^{2+} influx. Delayed rectifier potassium (Kv) channels play a crucial role in determining β-cell electrical activity since they repolarise action potentials and thereby limit Ca^{2+} channel activity. Since over-expression of Kv channels in β-cells leads to diabetes in transgenic animals, we have investigated the expression of Kv channel mRNAs and their function in insulin-secreting cells isolated from patients with hyperinsulinism.

All experiments were carried out *in vitro* using tissues obtained from control donors ($n = 6$), and patients with hyperinsulinism in infancy (HI) ($n = 11$) or insulinoma ($n = 1$). RNA was extracted from isolated tissues by standard protocols and, with specific oligonucleotide primers, RT-PCR was used to document the expression of α-subunit (Kv1.1 to 1.6, Kv2.1, 2.2, Kv3.1, 3.3, 3.4, Kv4.1 and 4.2) and β-subunit (Kvβ1.1, 2.1 and 3.1) mRNAs for human Kv channels. Functional data were obtained using the whole-cell patch-clamp techniques under standard conditions; Kv currents were evoked by holding the cells at −70 mV and applying a series of 10 mV step depolarisations of 500 ms duration from −60 mV to +80 mV. Results are expressed as means ± S.E.M. and the Mann-Whitney rank sum test was used to test for statistically significant differences.

Analysis of Kv channel mRNAs was undertaken and revealed the differential loss of several Kv channel subunit mRNAs in HI islets ($n = 3$). Specifically, we found that all HI islet preparations failed to express Kv3.3 and the Kvβ2.1 subunit, which is used as a chaperone protein for Kv channel α-subunits. Additionally, islets from one patient with a contiguous gene deletion of Ch11p15 also failed to express Kv3.1 mRNA. In control ($n = 40$ experiments) and patient tissues defined as either focal or diffuse HI ($n = 10$ patients, 56 experiments), Kv channel currents were readily recorded and exhibited similar peak current values in both tissues: 133 ± 9 pA pF^{-1} *vs.* 164 ± 12 pA pF^{-1} (n.s.) in control and HI, respectively. However, in one patient with an atypical form of HI in which K_{ATP} channel function was preserved, the magnitude of Kv currents was markedly reduced with respect to control values: 24 ± 6 pA pF^{-1} ($n = 6$, $P < 0.001$).

In summary we have documented the mRNA expression profiles and function of Kv channels in control human insulin-secreting cells and in tissues isolated from patients with hyperinsulinism in infancy. In typical HI β-cells, Kv channels are operational despite altered expression of mRNAs, but in those patients with non-typical disease where HI arises without K_{ATP} channel defects, our data suggest that defects in Kv channels may be related to the pathogenesis of HI.

All procedures accord with current local guidelines and the Declaration of Helsinki

PS P136

Identification and characterisation of a novel human small-conductance Ca^{2+}-activated K^+ channel splice variant

Matthew P. Burnham and Arthur H. Weston

School of Biological Sciences, University of Manchester, Manchester M13 9PT, UK

We report the identification and characterisation of a novel splice-variant of the human SK3 small-conductance Ca^{2+}-activated K^+ channel (SK_{Ca}).

Using the GenBank Expressed Sequence Tag (EST) database to identify SK_{Ca}-related sequences, a full-length cDNA was obtained from Raji cell RNA by a combination of 5′ and 3′ rapid amplification of cDNA ends (5′ and 3′ RACE). The predicted translation product differed from hSK3 in the N-terminus, with a novel sequence of five amino acids replacing the conventional N-terminal and first transmembrane segment. RT-PCR indicated that the novel sequence was expressed in kidney, lung and trachea among a panel of normal human tissues (obtained from Clontech), a distribution distinct from that of conventional hSK3. Subcloning the novel coding sequence into pcDNA3.1 mammalian expression vector and transfection of HEK cells resulted in expression of a V5 epitope-tagged protein. Immunofluorescence studies indicated that anti-V5 labelling was confined to the intracellular compartment, presumably the endoplasmic reticulum, and labelling was not evident at the plasmalemma. Co-expression with conventional hSK3 neither rescued the novel variant nor allowed its plasmalemmal expression, nor did the variant inhibit the robust plasmalemmal expression of hSK3. Current–voltage relationships, derived from whole-cell patch-clamp recordings (1 μM free calcium pipette solution) of cells transfected with the novel variant or co-transfected with hSK3, were indistinguishable from those recorded in the absence of the novel variant.

These data suggest that the novel hSK3 splice variant transcript identified in normal human tissues does express at the protein level when transfected into HEK cells. However, under these expression conditions, the protein does not form a plasmalemmal K^+ channel or associate with hSK3 subunits.

PS P137

An investigation of the role of positively charged S4 residues in the voltage-dependent gating of HERG potassium channels expressed in *Xenopus* oocytes

Rachael M. Hardman and John S. Mitcheson (introduced by N.B. Standen)

Department of Cell Physiology and Pharmacology, University of Leicester, Leicester LE1 9HN, UK

The human *ether-à-go-go-related* gene (HERG) encodes the pore-forming subunit of a cardiac potassium (K^+) channel involved in action potential repolarisation. HERG channel gating is characterised by very slow activation and fast C-type inactivation, which unlike other voltage-gated K^+ channels appears to be independent of activation. Thus, for wild-type (WT) HERG the potentials for half-maximal activation ($V_{0.5,act}$) and inactivation ($V_{0.5,inact}$) are -25 ± 0.7 mV and -85 ± 6 mV, respectively. Although S4 is assumed to be the voltage sensor for both gating processes, the contribution of each charged residue to gating is unknown. The aim of this study was to mutate each positively charged residue on S4 to an uncharged cysteine and investigate how this altered the activation and inactivation properties of HERG channels.

Two-electrode voltage clamp was used to record HERG currents from isolated *Xenopus* oocytes perfused with a Na^+-based solution containing 2 mM K^+ and 2 mM Ca^{2+}, pH 7.6, at room temperature. Currents were recorded 1–5 days after injection of cRNA for WT or S4 mutant channels. Mean (± S.E.M.) data are from more than five cells.

The voltage dependence of activation was determined from normalised peak tail currents measured at –70 or –140 mV, following 5 s depolarisations to potentials between –100 and +70 mV. Mutation of residues in the middle of the putative S4 domain resulted in positive shifts of $V_{0.5,act}$ of 31.5 ± 0.44, 47.6 ± 0.46 and 9 ± 1.12 mV for R528C, R531C and R534C, respectively, and no shifts of inactivation, measured using a triple pulse protocol. Cysteine substitutions at the ends of S4 had effects on both activation and inactivation gating. Mutation of R537 resulted in a -16.1 ± 1 mV shift of $V_{0.5,act}$ and $+35 \pm 6$ mV shift of $V_{0.5,inact}$. The mutations K525C and K538C resulted in substantial negative shifts of activation. Furthermore, in addition to a WT-like fast component of inactivation, a slower component was also identified. Tail currents following a depolarisation to +20 mV were smaller than at –40 mV, probably because of slow recovery from inactivation.

These data suggest that all six positively charged residues in the S4 domain of HERG contribute to voltage-dependent gating. The S4 mutant channels can be divided into two groups based on changes to gating. One group in the middle of S4 have positive shifts of activation and WT-like inactivation properties, whereas the mutants at the ends of S4 have negative shifts of activation and modified inactivation properties.

The results provide further evidence that HERG channel inactivation is independent of (or weakly coupled to) activation.

This work was supported by the Medical Research Council.

All procedures accord with current UK legislation